AGU Word Manuscript Template

Please use this template and for submitting a new or revised manuscript to any AGU journal. Using this template and following the guidelines below will help us expedite processing of your paper.

The template starts on page 2. Delete this cover page.

Helpful links:

Descriptions of individual journals and links to their submission sites are here: https://www.agu.org/Publish-with-AGU/Publish

Additional instructions are available under "How to Submit" in the link above.

Please follow our checklists for initial submission or revision. **Resubmissions that were previously reviewed should follow the "revision" checklist.**

AGU has implemented new styles. These mostly affect formatting of references, which are now cited in parentheses, not brackets. See here for details.

Length: Research Articles in most AGU journals have an allowed length of 25 publication units. Letters in *Geophysical Research Letters (GRL)* and Technical Reports on Data or Methods in *Earth and Space Science* have an **allowed length of 12 publication units (1 unit = 500 words or 1 table or figure; title, plain language summary, author lists, references, and all supplements are excluded from the word count).**
AGU encourages research publications that are thorough but also concisely presented. This benefits readers as well as reviewers, who are increasingly taxed. Editorial and production costs also scale with length. However, all AGU journals except *GRL* allow longer papers beyond these guidelines for an additional fee (**see table**) that reflects these incentives. ***Submissions to GRL that are longer than the allowed length of 12 Publication Units will be returned immediately for shortening.*** Some journals have publication fees. Open access is available in all AGU journals.

Please use the .docx format if possible (all versions of Word after 2007). This document contains pre-set styles that apply to each manuscript element. These styles are listed below. Please keep these styles by pasting in your text when done and matching, or applying these styles in your document using the style pane or organizer.

Title
Authors
Affiliation
Key points
Abstract
Plain Language Summary
Body Text
Headings (Main and secondary)
Figure or Table Captions
References

Please use our separate template for supporting information: https://www.agu.org/-/media/Files/Publications/AGUSupporting-Information_Word_template.docx?la=en&hash=BEA4EB05F3A8E5C18A2BAAC5BCCDBC9E33FFBC25

More specific formatting instructions are provided in the actual template, which follows. Delete these instructions from your finished manuscript.

AGU requires the corresponding author to register for an ORCid. Co-authors are also encouraged to register. We will note published contributions and reviews in your ORCid profile. Each author can easily create or link your ORCID in GEMS via Modify Profile/Password on the landing page.

Changes in the Elevation and Mass of Arctic Glaciers and Ice Caps, 2010 - 2017

(A title should be specific, informative, and brief. Capitalize major words in titles, but not conjunctions and articles. Use abbreviations only if they are defined in the abstract. Titles that start with general terms then specific results are optimized in searches—delete these notes when done)

P. Tepes[1], N. Gourmelen[1,2], P. Nienow[1], M. Tsamados[3], A. Shepherd[4], F. Weissgerber[1], and Lin Gilbert[3]

(List authors by first name or initial followed by last name and separated by commas. Use superscript numbers to link affiliations, and symbols *†‡ for author notes. For example, X. Jones[1]*, P. Smith[1,2] Authors are individuals who have significantly contributed to the research and preparation of the article. Group authors are allowed, if each author in the group is separately identified in an appendix.)

[1]School of GeoSciences, University of Edinburgh, UK.
[2]IPGS UMR 7516, Université de Strasbourg, CNRS, Strasbourg, France.
[3]Centre for Polar Observation and Modeling, University College London, London, UK.
[4]Centre for Polar Observation and Modelling, School of Earth and Environment, University of Leeds, Leeds, UK.

(Affiliations should be preceded by superscript numbers corresponding to the author list. Each affiliation should be run in so that the full affiliation list is a single paragraph.)

Corresponding author: Paul Tepes (paul.tepes@ed.ac.uk)

†Additional author notes should be indicated with symbols (current addresses, for example).

(include name and email addresses of the corresponding author. More than one corresponding author is allowed in this Word file and for publication; but only one corresponding author is allowed in our editorial system.)

Key Points:

- Arctic glaciers and ice caps lost 86 Gt a^{-1} between 2010 and 2017, a sustained rate of loss from the previous decade
- 87% of this loss is due to surface mass balance and 13% is due to anomalous discharge
- Increased ice discharge accounts for 43% of total mass loss anomaly in the Barents and Kara seas, coinciding with warming and sea-ice decline

(Key Points summarize the main points and conclusions of the article. Each must be 140 characters or less with no special characters or acronyms. The above elements should be on a title page.)

Abstract

Arctic glaciers and ice caps (GIC) are retreating, rapidly, due to polar amplification of climate warming, and this is expected to continue over the 21st century. Here, we use CryoSat-2 swath interferometric altimetry to show that they thinned by 0.25 m a^{-1} ± 0.03 m/yr, on average, between 2010 and 2017, and lost 609 ± 18 Gt of ice. By modelling elevation trends over land-terminating glaciers, we estimate that 87 % of all thining was due to changes in surface mass balance, and the remainder was due changes in ice flow. Tidewater glaciers discharging into the Barents and Kara Seas have speeded up as the regional atmosphere and ocean have warmed, and glacier dynamics now accounts for 43 % of ice loss from this sector. Altogether, Arctic GIC now contribute 0.24 ± 0.01 mm/yr to global sea level rise.

Plain Language Summary

Global heating is causing Arctic glaciers and ice caps to shrink, but exactly how they respond to atmospheric and oceanic warming remains unclear. We measure changes in the volume of over 15 thousand glaciers in seven regions across the Arctic and estimate how much ice they have lost from their surface (due to snowfall and ice melting) and through speedup of glaciers flowing into the ocean. Altogether, the glaciers we have surveyed lost enough ice between 2010 and 2017 to cause a 2-millimeter rise in global sea levels. The vast majority (87 %) of this ice loss was due to changes in snowfall and runoff at glacier surfaces. However, some marine-terminating glaciers in the Russian Arctic and in Svalbard are flowing faster than they used to because the local climate has warmed, and these glaciers are responsible for almost half (43 %) of ice loss from these regions.

1. Introduction

Arctic glaciers and ice caps (GIC) play a key role in local freshwater budgets, impact thermohaline circulation in the North Atlantic (Thornalley et al., 2018; Yang et al., 2016), and are a significant contributor to sea level rise (Zemp et al., 2019; Gardner et al., 2013; Ciraci et al., 2020). They store 40 % of global GIC ice volume (Farinotti et al., 2019), and their losses are increasing as atmospheric and oceanic temperatures rise (Barton et al., 2018; Ding et al., 2014) and as Arctic sea ice cover shrinks (Onarheim et al., 2018). Although projections of ice loss due to changes in surface mass balance (*SMB*) are relatively mature, the dynamic response of land ice to climate forcing constitutes the main uncertainty in global sea level projections (Church, 2013; Martin and Adcroft, 2010). However, few estimates of ice losses due to anomalous glacier discharge (*D*) exist for Arctic GIC – in part due to the coarse spatial resolution or sparse sampling of previous surveys.

Commented [GN1]: Need to add reference

Trends in Arctic GIC *SMB* have been driven by large-scale atmospheric circulation patterns across the Arctic (Delhasse et al., 2018) and by CO_2-induced radiative forcing (Byrne and Schneider, 2018; Shindell and Faluvegi, 2009). In addition, Arctic GIC mass loss has been amplified in recent years by accelerated ice discharge from marine-terminating (tidewater) glaciers which have been destablised (Nuth et al., 2019; Willis et al., 2018; Strozzi, Kääb, et al., 2017; McMillan et al., 2014). However, the respective roles of internal processes (i.e. glacier surges) and external forcing in driving ice dynamical instabilities remains unclear (Dunse et al., 2015; McMillan et al., 2014). Here, we use CryoSat-2 swath interferometric altimetry (Gourmelen et al., 2018; Foresta et al.,

2016) to measure changes in the elevation and mass of Arctic GIC between 2010 and 2017 and with a spatial resolution (500 m) and density (68 %) that is fine enough to discriminate between changes due to *SMB* and *D*.

2. Arctic GIC Elevation Change

We derive rates of change in land ice surface elevation $\dot{h}$ in all areas of the Arctic beyond Greenland (Figure 1). This includes the southern and northern Canadian Arctic Archipelagos (CAA-S and CAA-N, respectively), Iceland (Ic), Svalbard (Sv), and the Russian Arctic Archipelagos (RAA) of Franz Joseph Land (FJL), Novaya Zemlya (NZ) and Severnaya Zemlya (SZ) (Figure 1). We apply swath processing to CryoSat-2 altimetry data spanning the period 2010-2017 to retrieve time-dependent elevation measurements over the GIC (Gourmelen et al., 2018 and supplementary informations). Elevation change $\dot{h}$ is computed using a plane-fit algorithm for the entire measurement period, 2010-2017 on a 500m by 500m posting as a function of easting *(x)*, northing *(y)*, and time *(t)*:

$$h(x, y, t) = c_0\, x + c_1\, y + c_2\, t + c_3 = \nabla h(x, y) + \dot{h} t + c$$

where

$$\nabla h(x, y) = \frac{\partial h}{\partial x} x + \frac{\partial h}{\partial y} y \qquad \text{and} \qquad \dot{h} = \frac{\partial h}{\partial t}$$

$\nabla h(x, y)$ is the ice surface gradient, and the time-dependent coefficient c_2 retrieved from the linear fit is the rate of surface elevation change $\dot{h}$.

The CryoSat-2 high-measurement density over the Arctic translates into a ratio of measured-to-total glaciated area equal to 83% over the GIC of the RAA, 79% over Sv and Ic, and 60% over the CAA, with good coverage over the ice margins (Table 1, Fig. S1). Ice thinning is widespread across the Arctic, and the median rate of elevation change is -0.25 m a^{-1}. There is, however, considerable spatial variability, and the 5% and 95% quantiles are -1.65 m a^{-1} and +0.70 m a^{-1} respectively, reflecting the diversity of responses of ice masses to forcing across the Arctic (Fig. 1).

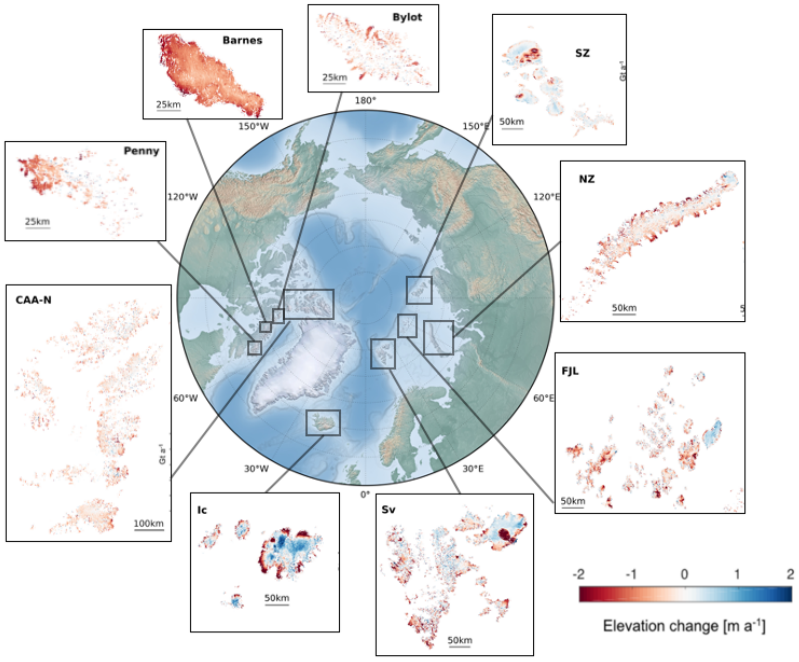

Figure 1. Rates of surface elevation change [m a^{-1}] of the Arctic GIC included in this study.

The climate of the CAA exhibits low inter-annual variability in precipitation but high variability in summer surface temperatures (Gardner et al., 2012), which results in spatially homogenous thinning patterns, driven largely by changes in summer surface melt rates (Gardner et al., 2011, 2012). Median thinning rates over CAA-S (0.75 m a^{-1}) are three times larger than over CAA-N (0.24 m a^{-1}), reflecting the latitudinal control on *SMB*. Rates of thinning of up to 5 m a^{-1} are observed at low elevations and over a limited number of marine-terminating outlet glaciers, including on Devon Ice Cap and Prince of Wales Icefield. The strongest spatially extensive thinning signal across CAA-S is from the ablation zone of Barnes and Penny Ice Caps where thinning rates are in excess of 2.5 m a^{-1} (Fig. 1). Icelandic ice caps display diverse patterns of glacier change (Fig. 1), reflecting in part their location over volcanically active terrain, frequent surges, and high variability in weather patterns (Foresta et al., 2016). Nevertheless, between 2010 and 2017, they have mainly experienced *SMB*-driven ice loss, with strong seasonal trends and high melt rates of up to 6 m a^{-1} along ice cap margins and thickening in the accumulation zones driven by post-surge dynamic responses and exceptionally large winter accumulation in recent years (Wouters et al., 2019; Foresta et al., 2016).

Complex patterns of change also prevail over the archipelagos of the Barents and Kara Sea (BKS) region where rates of $\dot{h}$ have high spatial variability (Fig. 1). Pronounced thinning is observed at a large number of marine-terminating glacier catchments, which represent 58% of the glaciated area

of all Arctic archipelagos east of Greenland. Examples of thinning include an increasing number of marine-terminating basins in Sv, such as along the SE flanks of Austfonna Ice Cap, including Basin 3 (McMillan et al., 2014), and the frontal destabilisation of Stonebreen, Edgeøya (Strozzi, Kääb, et al., 2017). In SZ, six basins are thinning at an average rate (0.85 m a^{-1}) an order of magnitude higher than the rest of the archipelago (0.08 m a^{-1}), all six of which are marine-terminating catchments located primarily around the southern and eastern flanks of the Academy of Sciences Ice Cap (Moholdt, Heid, et al., 2012), and one on the western flank of Vavilov Ice Cap (Willis et al., 2018). Fed by ice streams from the Karpinsky and Rusanov Ice Caps, the collapse of the Matusevich Ice Shelf in 2012 triggered the rapid acceleration of two main outlet glaciers of Karpinsky Ice Cap, one having sped up by up to 200% at its terminus between 2010 and 2014 (Willis et al., 2015). Windy Ice Cap on Graham Bell Island, the easternmost ice cap in FJL, represents a singularity in the archipelago, thickening at an average rate of 0.4 m a^{-1}, thereby maintaining a positive trend since the 1950s (Moholdt, Wouters, et al., 2012).

3. Arctic GIC Mass Balance

We compute Arctic GIC volume changes using our elevation rates and glacier area extents from the Randolph Glacier Inventory (RGI 6.0), and we estimate their mass balance m using an assumed constant density of ice equal to 850 ± 60 kg m^{-3} (Huss, 2013) and by applying a regionalization scheme (See supplementary information and table S1). Between 2010 and 2017, Arctic GIC outside of Greenland lost on average 87.0 ± 2.6 Gt of ice per year (Table 1), corresponding to a mean sea level contribution of +0.283 ± 0.009 mm a^{-1}. The largest losses occurred over the CAA with mass trends of -32.3 ± 1.6 Gt a^{-1} and -24.8 ± 1.8 Gt a^{-1} for CAA-N and CAA-S, respectively. The largest loss per unit area is for CAA-S (606 ± 44 kg m^{-2} a^{-1}), followed by Sv (401 ± 24 kg m^{-2} a^{-1}), NZ (385 ± 18 kg m^{-2} a^{-1}), CAA-N (308 ± 15 kg m^{-2} a^{-1}), FJL (297 ± 23 kg m^{-2} a^{-1}), and Ic (234 ± 18 kg m^{-2} a^{-1}). over SZ (-106 ± 6 kg m^{-2} a^{-1}) is the lowest in the Arctic, representing ~1/4 of the rate of loss over NZ and ~1/3 that of FJL (See supplementary table S2 for complete specific mass balance record).

Table 1. Mass budget (m), surface mass balance (SMB), discharge anomaly (D), and sea level contribution (SLR) of Arctic GIC other than those surrounding Greenland. Also shown are the subsurface ocean temperature (SOT) anomalies relative to the reference period (1990-2009) mean. Area is from RGI 6.0. Mb 2003-2009 is from Gardner et al. (2013) for RAA, Sv, Ic, CAA-N and CAA-S, and Moholdt et al. (2012) for NZ, SZ and FJL, the latter covering the period 2004–2009. SOT is from TOPAZ. A_t and A_o are total area and area observed respectively.

Region	A_t*	# Glaciers	A_o	m	m	SLR	SMB	D	D/m	DSOT
	[10^3 km^2]		(%)	[Gt a^{-1}]	[Gt a^{-1}]	[mm a^{-1}]	[Gt a^{-1}]	[Gt a^{-1}]	(%)	(°C)
				2003-09	2010-17	2010-17	2010-17	2010-17	2010-17	2010-17
FJL	12.8	1069	83	-0.6 ± 0.9	-3.8 (-4.0) ± 0.3	-0.010 ± 0.001	-1.1 ± 0.1	-2.7 ± 0.6	72	0.3
NZ	22.1			-7.1 ± 1.2	-8.5 (-9.0) ± 0.4	-0.024 ± 0.001	-7.4 ± 0.3	-1.1 ± 0.5	13	0.6
SZ	16.0			-1.4 ± 0.9	-1.7 (-1.8) ± 0.1	-0.005 ± 0.000	-0.1 ± 0.0	-1.6 ± 0.2	94	0.1
Sv	33.2	1615	79	-5 ± 2	-13.3 (-14.1) ± 0.8	-0.037 ± 0.002	-7.1 ± 0.4	-6.2 ± 0.9	47	0.7
Ic	11.1	568	79	-10 ± 2	-2.6 (-2.8) ± 0.2	-0.007 ± 0.001	-2.6 ± 0.2	-	-	0.3

CAAN	105.0	4556	60	-33 ± 4	-32.3 (-34.2) ± 1.6	-0.089 ± 0.004	-32.6 ± 1.6	+0.3 ± 1.4	-1	-0.2
CAAS	40.9	7415		-27 ± 4	-24.8 (-26.3) ± 1.8	-0.068 ± 0.005	-25.1 ± 1.8	+0.3 ± 0.4	-1	-0.2
Total	**241.1**	**15223**	**68**	**-86 ± 7**	**-87.0 (-92.1) ± 2.6**	**-0.240 ± 0.007**	**-76 ± 2.3**	**-11.0 ± 1.9**	**13**	
RAA	50.9	1069	83	-11 ± 4	-14.0 (-14.8) ± 0.5	-0.039 ± 0.001	-8.6 ± 0.3	-5.4 ± 0.8	38	0.4
BKS	84.1	2684	81	-16 ± 4	-27.3 (-28.9) ± 0.9	-0.075 ± 0.002	-15.7 ± 0.5	-11.6 ± 1.2	43	0.5
CAA	145.9	11971	60	-60 ± 6	-57.1 (-60.5) ± 2.4	-0.158 ± 0.007	-57.7 ± 2.4	+0.6 ± 1.5	-1	-0.2

Our measurements (Table 1 and Figure 2) reveal a sustained ice loss between 2010 and 2017 compared with the previous 2003-2009 period (Gardner et al., 2013). However, this overall mass loss hides contrasting patterns of change across the regions. While during 2010-2017, the CAA has seen a rate of loss comparable to the period between 2003 and 2009, Ic glaciers have lost mass at a lower rate, due primarily to recent record rates of winter accumulation leading locally to positive *SMB* (Wouters et al., 2019; Foresta et al., 2016). Our estimates for Ic are significantly lower than a recent GRACE estimate (Ciraci et al., 2020) but are in agreement with another recent GRACE estimate (wouters et al., 2019) and a field-based estimate (Zemp et al., 2019). The largest increase in rates of mass loss occurred within the BKS sector. Ice loss over Sv, for example, almost trebled over the CryoSat-2 measurement period (13.3 ± 0.8 Gt a^{-1}) compared to the previous six years (Gardner et al., 2013).

In the RAA, FJL has seen a six-fold increase in mean annual losses during 2010-2017 (3.8 ± 0.3 Gt a^{-1}) compared to the 2004-2009 period (0.6 ± 0.9 Gt a^{-1}, Table 1). NZ remained the largest contributor to sea level change in this region, losing 8.5 ± 0.4 Gt a^{-1} between 2010 and 2017. This is 27% more ice loss per year compared to 2004-2009 (Moholdt, Wouters, et al., 2012), and 80% more than the 60-year average (5.1 ± 0.8 Gt a^{-1}) (Melkonian et al., 2016). SZ's rate of loss was similar (29% increase) to the previous decade, reaching 1.7 ± 0.1 Gt a^{-1} in 2010-2017 (Table 1). Overall, GIC within the BKS sector have released an extra 100 km^3 of freshwater to the ocean between 2010 and 2017 compared to the previous decade, a volume similar in magnitude to that associated with receding sea ice cover in this region (Labe et al., 2018; Onarheim et al., 2018).

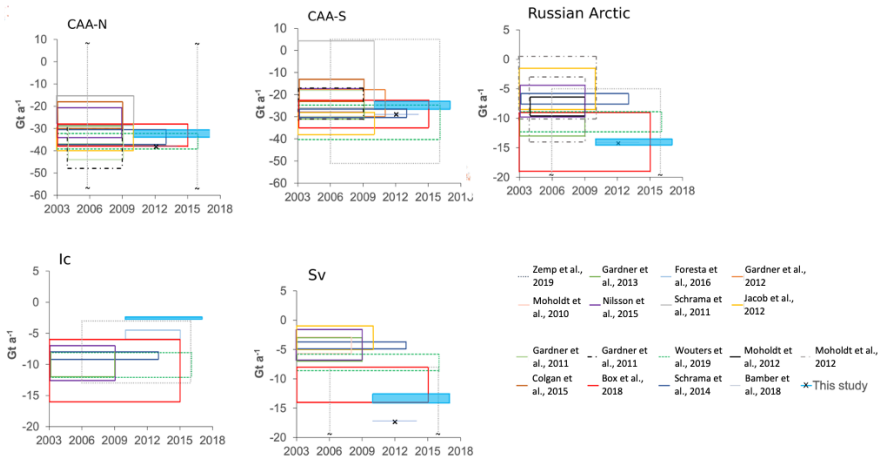

Figure 2: Summary of regional total mass balance. Mass balance is represented in graphical form as boxes indicating average values over a given study period (width) with error estimates (height).

4. Surface Mass Balance and Glacier Dynamics

Over land-terminating sector, local value of $\dot{h}$ can be related to the local *SMB* anomaly, that is the difference between the *SMB* and emergence and submergence flux (Figure 3a). We thereby assume that land-terminating basins are dominated by surface processes and hence dynamic thickness changes are either negligible, or uniform across the region as defined for the purpose of the analysis. Integrated over an entire basin, $\dot{h}$ is equal to *SMB*. To quantify the relative contribution of *SMB* and *D* to the overall mass loss, we parametrize thinning $\dot{h}$ as a function of first order controls on SMB, that is elevation (h_l), and spatial coordinates (x_l, y_l). We solved for the parameters' coefficients over land-terminating GIC basins only, for each of the seven regions (see Table 2 for coefficients):

$$\dot{h}_l \approx a_0 {h_l}^3 + a_1 {h_l}^2 + a_2 h_l + a_3 x_l + a_4 y_l + a_5$$

We then use our parametrization to *i)* estimate a bulk SMB_m over marine-terminating sectors, and *ii)* derive a bulk *D* by subtracting SMB_m from the total marine-terminating GIC mass balance. A comparison between our derived SMB_l and that of the regional atmospheric climate model RACMO2.3 over land-terminating sectors for the Canadian Arctic (Noel et al., 2018) demonstrates an excellent agreement (Figure 3b). It also highlights the ability of our parametrisation to capture the first order *SMB* dependency on elevation and geographical location resulting in *SMB* variability between land- and adjacent marine-terminating sectors, and to therefore accurately determine marine-terminating bulk SMB_m (See supporting information).

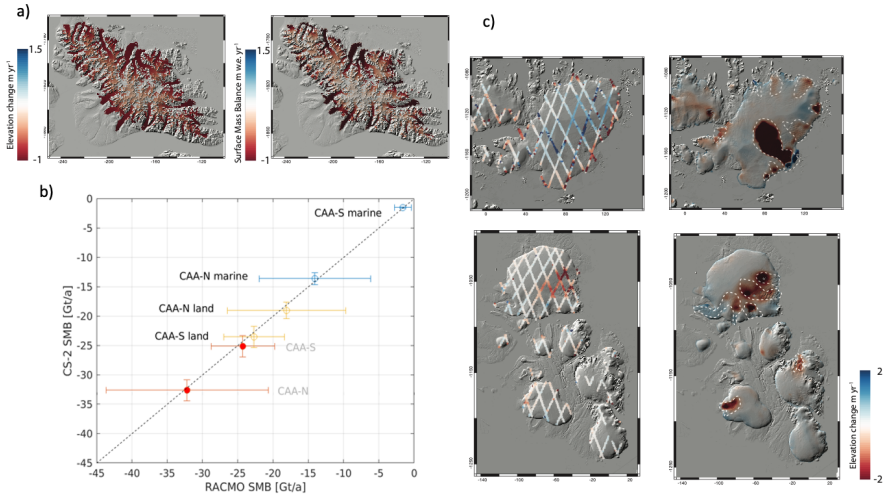

Figure 3: a) CryoSat-derived SMB anomaly model (left) versus RACMO SMB (right) over Bylot island; b) CryoSat and RACMO2.3 derived SMB across the Canadian Arctic: all regions (red), land-terminating sectors (yellow), marine-terminating sectors (blue); c) IceSat rates of elevation change (left) and dynamic thinning (MB minus SMB_m) over Austfonna and Severnaya Zemlya, dashed line indicate the location of major flow units (right).

Across the surveyed GIC, SMB is responsible for 87% of mass loss while anomalous discharge accounts for 13%. There are, however, strong regional differences, as well as differences in the spatial trends of *SMB* and *D* (Table 1, Figure 4, Fig. S2). In the CAA, our results confirm that *SMB* dominates the total mass imbalance of GIC west of Greenland, with decreasing contribution from *D* since 1990 (Mortimer et al., 2018; Millan et al., 2017), while the BKS sector show the strongest impact of dynamic loss. We observe an increasingly negative area-specific *SMB* with distance from the pole (Fig. S2b) (Noel et al., 2018). In contrast, a simple latitudinal control on *SMB* is not apparent across the archipelagos east of Greenland, reflecting the more complex interplay between atmospheric and oceanic influences. Noteworthy are the Sv-FJL-SZ and NZ-SZ gradients of *SMB,* with less negative values in north-eastward direction resulting from decreasing incursions of hot, moist Atlantic air masses (Moholdt, Wouters, et al., 2012).

Between 2010 and 2017, ice losses in the BKS sector were nearly two times larger per unit area from marine-terminating (384 ± 16 kg m^{-2} a^{-1}) than from land-terminating basins (209 ± 10 kg m^{-2} a^{-1}), a disparity that has clearly increased compared to the previous decade, as revealed by the acceleration of tidewater glaciers in recent years (Nuth et al., 2019; Strozzi, Paul, et al., 2017). This increase can be attributed largely to the rapid deflation of a small number of marine-terminating basins (Nuth et al., 2019; Willis et al., 2018; Strozzi, Kääb, et al., 2017; Dunse et al., 2015; McMillan et al., 2014). Austfonna Ice Cap alone lost 4.6 ± 0.3 Gt a^{-1} during 2010-2017, a budget dominated by the dynamic activation of Basin 3 since 2012 (McMillan et al., 2014). In SZ, where *SMB* represents only 6% of total mass loss, ice dynamics were largely responsible for the negative regional losses between 2010 and 2017 (Table 1).

It is striking to observe that all major flow units in Austfonna and SZ are currently dynamically thinning, which was the case during the IceSat period (Figure 3c). Elsewhere in the BKS sector, increased ice discharge accounted for 72%, 47% and 13% of the total mass loss for FJL, Sv and NZ respectively. By unit area, FJL, Sv and SZ exhibit the largest rates of dynamic loss *D* with 212± 49 kg m^{-2} a^{-1}, 188 ± 30 kg m^{-2} a^{-1} and 98 ± 11 kg m^{-2} a^{-1}, respectively. Some of NZ's Barents Sea coast outlet glaciers accelerated during the study period (Carr et al., 2017; Melkonian et al., 2016), contributing to a dynamic imbalance of -51 ± 29 kg m^{-2} a^{-1}. By unit marine-terminating basin area, which highlights the intensity of dynamic instability, Sv lost ice *via* discharge at 277 ± 41 kg m^{-2} a^{-1} owing to Basin 3, followed by FJL at 235 ± 54 kg m^{-2} a^{-1}, SZ at 205 ± 20 kg m^{-2} a^{-1} and NZ at 82 ± 37 kg m^{-2} a^{-1}.

5. Drivers of ice loss

Although atmospheric warming is the primary cause of ice loss from the surface of Arctic GIC through increased melting (Ding et al., 2014), a broad range of factors affect their discharge. Tidewater glaciers are influenced by any change in their boundary conditions, as these can trigger dynamic instabilities that are able to propagate rapidly inland and lead to significant loss of ice (Nuth et al., 2019; Willis et al., 2018; Dunse et al., 2015; McMillan et al., 2014). In the Arctic, the influx of Atlantic Ocean water, the recirculation of warm bottom water in fjords, the rapid drainage of surface meltwater to the base of glaciers, submarine melting driven by the buoyant advection of subglacial discharge at glacier calving fronts, and changes in sea ice conditions within fjords are all known to affect rates of tidewater glacier flow (Slater et al., 2016; Cook et al., 2019; Cowton et al., 2018; Robel, 2017). To investigate the drivers of the recent Arctic GIC dynamical imbalance (Table 1), we analysed trends in the regional atmosphere (Dee et al., 2011) and ocean (Xie et al., 2017) temperatures and in sea ice concentration (Comiso et al., 2017).

The Arctic climate has warmed, significantly, and mean air temperatures were 0.9 to 3.4 °C higher during our survey period than in the preceding two decades (See supplementary table S3*)*. However, while atmospheric warming has occurred across the region as a whole, ocean warming and sea ice retreat have been largely restricted to sectors east of Greenland–where GIC have experienced significantly increased glacier discharge (*Figure 4*). For example. across the BKS sector – including Sv, NZ, FJL, and SZ - the average rise in sea surface, subsurface ocean, and atmospheric temperatures adjacent to its GIC have been 0.6, 0.5, and 2.6 °C, respectively, and the average reduction in sea ice concentration has been 12.4%. By comparison, the ocean temperature and sea ice concentration around the CAA region have changed little.

The warming of the BKS sector has been associated with the combined effects of enhanced storm activity and increased Atlantic Water inflow to the Siberian Shelf seas (Barton et al., 2018; Lind et al., 2018; Polyakov et al., 2017). Close to half (43 %) of the sectors GIC loss is due to increased ice discharge, and there is a moderate (r=0.72) correlation with the contemporaneous increase in subsurface ocean temperature (Table 1) – and an even stronger (r=0.88) correlation when the alpine glaciers of NZ are excluded. This coupling provides a simple link between the dynamical imbalance of GIC and the regional environmental change. Farther afield, it has been shown that the Arctic- and North Atlantic Oscillations are correlated with glacier mass balance (Wouters et al., 2019; Bjørk et al., 2018; Carr et al., 2017; Ding et al., 2014; Moholdt, Wouters, et al., 2012; Gardner and Sharp, 2006; Zeeberg and Forman, 2001), with opposite effects in the eastern and

western Hemispheres depending on the position and strength of the Arctic Circumpolar Vortex (Wouters et al., 2019; Bjørk et al., 2018; Gardner and Sharp, 2006).

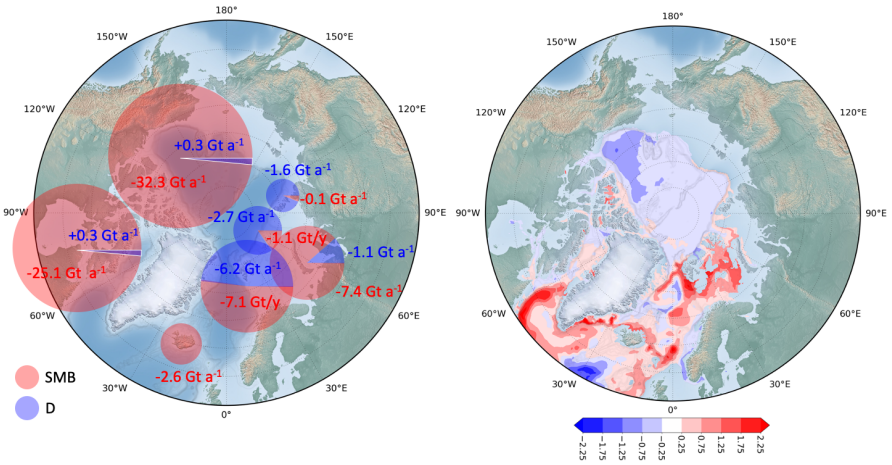

Figure 4: a) Mass balance partitioned between SMB and discharge anomaly D. b) SOT anomaly between the CryoSat-2 period (2010-2017) and the reference period (1990-1999). SOT is 200m depth ocean temperature from TOPAZ.

4. Conclusions

Using CryoSat-2 swath radar altimetry, we have computed elevation and mass trends for all Arctic GIC outside Greenland with unprecedented (500 m) spatial resolution. Between 2010 and 2017 we estimate they have lost 86 ± 7 Gt/yr of snow and ice, on average, a 7% increase relative to the 2003-2009 mean [Gardner et al., 2013] but with significant regional differences. By modelling the contribution due to SMB, we isolate the elevation change signal due to anomalous glacier flow. Using this approach, we find that SMB is responsible for the vast majority (87%) of the observed mass loss, while increased ice discharge has caused the remainder (13%). However, anomalous ice discharge from GIC in the Barents and Kara sea area has increased since the 2003-2009 period, and now accounts for 43% of the mass loss from this region. This enhanced dynamic signal has been occurring in conjunction with increased air and ocean temperature, and loss of sea-ice.

It is predicted that, even when excluding the mass balance of tidewater glaciers, losses from the CAA and the BKS will be dominating glacier change in future climate scenarios (Möller et al., 2016; Radić et al., 2014). Most importantly, while *SMB* is projected to be the prevalent mechanism of Greenland ice loss in the coming decades (Enderlin et al., 2014; Nick et al., 2013; Price et al., 2011), a recent study finds that *D, not SMB* has dominated ice losses in Greenland over the past half-century (Mouginot et al., 2019). Our results show that the dynamic response of marine-terminating GIC to climate forcing makes up a significant proportion of the total mass budget in the rest of the Arctic since 2010. This pattern is likely to endure over time, as the large number of Arctic tidewater glaciers will continue to respond to receding sea ice and to the impinging Atlantification of Arctic Ocean basins.

(All figures and tables should be cited in order. For initial submission, please embed figures, tables, and their captions within the main text near where they are cited. At revision, figures should be uploaded separately, as we need separate files for production. Tables and all captions should be moved to the end of the file.)

References should use a name-date format, not numbers. Enclose citations in parentheses with authors in upright text (non italics) as in: (Smith et al., 2009) or Smith et al. (2009). More information on in-text citations can be found in our Brief Style Guide,"Reference Formatting."

Acknowledgments

This work was performed under the European Space Agency (ESA) Support to Science Elements CryoSat+ CryoTop contract 4000107394/12/I-NB, CS+ Mountain Glaciers contract 4000114224/15/I-SBo to N.G. The authors would like to thank ESA for providing open access to CryoSat-2 data, NASA for providing access to Operation Ice Bridge, and Dr. B.P.Y. Noël for access to RACMO2.3 data.

Data

CryoSat-2 data can be downloaded from ftp://science-pds.cryosat.esa.int (accessed on 27/06/2019); NASA Operation Ice Bridge validation data is available for download at https://nsidc.org/data/icebridge (accessed on 27/06/2019); ice and snow masks for all regions except Iceland were taken from https://www.glims.org/RGI/rgi60_dl.html (accessed on 27/06/2019); RACMO data is available for download at https://doi.pangaea.de/10.1594/PANGAEA.881315; the passive microwave NASA Team and Bootstrap concentration data are available respectively from http://nsidc.org/data/nsidc-0051 and http://nsidc.org/data/nsidc-0079; The TOPAZ ARCTIC_REANALYSIS_PHYS_002_003 product is available from http://marine.copernicus.eu/services-portfolio/access-to-products; the ERA-Interim monthly means of daily means product is available from https://apps.ecmwf.int/datasets/.

References

1. Q. Yang, *et al.*, Recent increases in Arctic freshwater flux affects Labrador Sea convection and Atlantic overturning circulation. *Nat. Commun.* **7**, 10525 (2016).
2. D. J. R. Thornalley, *et al.*, Atlantic overturning during the past 150 years. *Nature* **556**, 227–230 (2018).
3. M. Zemp, *et al.*, Global glacier mass changes and their contributions to sea-level rise from 1961 to 2016. *Nature* **568**, 382–386 (2019).
4. A. S. Gardner, *et al.*, A reconciled estimate of glacier contributions to sea level rise: 2003 to 2009. *Science* **340**, 852–857 (2013).
5. D. Farinotti, *et al.*, A consensus estimate for the ice thickness distribution of all glaciers on Earth. *Nat. Geosci.* **12**, 168–173 (2019).
6. Q. Ding, *et al.*, Tropical forcing of the recent rapid Arctic warming in northeastern Canada and Greenland. *Nature* **509**, 209–212 (2014).
7. B. I. Barton, Y.-D. Lenn, C. Lique, Observed atlantification of the Barents Sea causes the Polar Front to limit the expansion of winter sea ice. *J. Phys. Oceanogr.* **48**, 1849–1866 (2018).
8. I. H. Onarheim, T. Eldevik, L. H. Smedsrud, J. C. Stroeve, Seasonal and regional

manifestation of Arctic sea ice loss. *J. Clim.* **31**, 4917–4932 (2018).
9. T. Martin, A. Adcroft, Parameterizing the fresh-water flux from land ice to ocean with interactive icebergs in a coupled climate model. *Ocean Model.* **34**, 111–124 (2010).
10. J. A. et al. Church, "Climate Change 2013: The Physical Science Basis. Contribution of Working Group I to the Fifth Assessment Report of the Intergovernmental Panel on Climate Change (IPCC)" (2013).
11. J. Mouginot, *et al.*, Forty-six years of Greenland Ice Sheet mass balance from 1972 to 2018. *Proc. Natl. Acad. Sci.* **116**, 9239–9244 (2019).
12. A. Delhasse, X. Fettweis, C. Kittel, C. Amory, C. Agosta, Brief communication: Impact of the recent atmospheric circulation change in summer on the future surface mass balance of the Greenland Ice Sheet. *Cryosphere* **12**, 3409–3418 (2018).
13. D. Shindell, G. Faluvegi, Climate response to regional radiative forcing during the twentieth century. *Nat. Geosci.* **2**, 294–300 (2009).
14. M. P. Byrne, T. Schneider, Atmospheric dynamics feedback: concept, simulations and climate implications. *J. Clim.* **31**, 3249–3264 (2018).
15. M. McMillan, *et al.*, Rapid dynamic activation of a marine-based Arctic ice cap. *Geophys. Res. Lett.* **41**, 8902–8909 (2014).
16. M. J. Willis, *et al.*, Massive destabilization of an Arctic ice cap. *Earth Planet. Sci. Lett.* **502**, 146–155 (2018).
17. C. Nuth, *et al.*, Dynamic vulnerability revealed in the collapse of an Arctic tidewater glacier. *Sci. Rep.* **9**, 5541 (2019).
18. T. Strozzi, A. Kääb, T. Schellenberger, Frontal destabilization of Stonebreen, Edgeøya, Svalbard. *Cryosphere* **11**, 553–566 (2017).
19. I. V. Polyakov, *et al.*, Greater role for Atlantic inflows on sea-ice loss in the Eurasian Basin of the Arctic Ocean. *Science* **356**, 285–291 (2017).
20. T. Dunse, *et al.*, Glacier-surge mechanisms promoted by a hydro-thermodynamic feedback to summer melt. *Cryosphere* **9**, 197–215 (2015).
21. T. R. Cowton, A. J. Sole, P. W. Nienow, D. A. Slater, P. Christoffersen, Linear response of east Greenland's tidewater glaciers to ocean/atmosphere warming. *Proc. Natl. Acad. Sci.* **115**, 7907–7912 (2018).
22. L. Foresta, *et al.*, Surface elevation change and mass balance of Icelandic ice caps derived from swath mode CryoSat-2 altimetry. *Geophys. Res. Lett.* **43**, 12138–12145 (2016).
23. N. Gourmelen, *et al.*, CryoSat-2 swath interferometric altimetry for mapping ice elevation and elevation change. *Adv. Sp. Res.* **62**, 1226–1242 (2018).
24. A. Gardner, G. Moholdt, A. Arendt, B. Wouters, Accelerated contributions of Canada's Baffin and Bylot Island glaciers to sea level rise over the past half century. *Cryosph.* **6**, 1103–1125 (2012).
25. A. S. Gardner, *et al.*, Sharply increased mass loss from glaciers and ice caps in the Canadian Arctic Archipelago. *Nature* **473**, 357–360 (2011).
26. B. Wouters, A. S. Gardner, G. Moholdt, Global glacier mass loss during the GRACE satellite mission (2002-2016). *Front. Earth Sci.* **7**, 96 (2019).
27. G. Moholdt, T. Heid, T. Benham, J. A. Dowdeswell, Dynamic instability of marine-terminating glacier basins of Academy of Sciences Ice Cap, Russian High Arctic. *Ann. Glaciol.* **53**, 193–201 (2012).
28. M. J. Willis, A. K. Melkonian, M. E. Pritchard, Outlet glacier response to the 2012 collapse of the Matusevich Ice Shelf, Severnaya Zemlya, Russian Arctic. *J. Geophys. Res.*

Earth Surf. **120**, 2040–2055 (2015).
29. G. Moholdt, B. Wouters, A. S. Gardner, Recent mass changes of glaciers in the Russian High Arctic. *Geophys. Res. Lett.* **39**, L10502 (2012).
30. M. Huss, Density assumptions for converting geodetic glacier volume change to mass change. *Cryosph.* **7**, 877–887 (2013).
31. A. K. Melkonian, M. J. Willis, M. E. Pritchard, A. J. Stewart, Recent changes in glacier velocities and thinning at Novaya Zemlya. *Remote Sens. Environ.* **174**, 244–257 (2016).
32. Z. Labe, G. Magnusdottir, H. Stern, Variability of Arctic sea ice thickness using PIOMAS and the CESM Large Ensemble. *J. Clim.* **31**, 3233–3247 (2018).
33. B. Noël, *et al.*, Six decades of glacial mass loss in the Canadian Arctic Archipelago. *J. Geophys. Res. Earth Surf.* **123**, 1430–1449 (2018).
34. R. Millan, J. Mouginot, E. Rignot, Mass budget of the glaciers and ice caps of the Queen Elizabeth Islands, Canada, from 1991 to 2015. *Environ. Res. Lett.* **12**, 024016 (2017).
35. C. A. Mortimer, M. Sharp, W. Van Wychen, Influence of recent warming and ice dynamics on glacier surface elevations in the Canadian High Arctic, 1995–2014. *J. Glaciol.* **64**, 450–464 (2018).
36. T. Strozzi, F. Paul, A. Wiesmann, T. Schellenberger, A. Kääb, Circum-arctic changes in the flow of glaciers and ice caps from satellite SAR data between the 1990s and 2017. *Remote Sens.* **9**, 947 (2017).
37. J. R. Carr, H. Bell, R. Killick, T. Holt, Exceptional retreat of Novaya Zemlya's marine-terminating outlet glaciers between 2000 and 2013. *Cryosph.* **11**, 2149–2174 (2017).
38. D. A. Slater, D. N. Goldberg, P. W. Nienow, T. R. Cowton, Scalings for submarine melting at tidewater glaciers from buoyant plume theory. *J. Phys. Oceanogr.* **46**, 1839–1855 (2016).
39. A. A. Robel, Thinning sea ice weakens buttressing force of iceberg mélange and promotes calving. *Nat. Commun.* **8**, 14596 (2017).
40. S. Lind, R. B. Ingvaldsen, T. Furevik, Arctic warming hotspot in the northern Barents Sea linked to declining sea-ice import. *Nat. Clim. Chang.* **8**, 634–639 (2018).
41. P. G. Myers, N. Kulan, M. H. Ribergaard, Irminger water variability in the West Greenland Current. *Geophys. Res. Lett.* **34**, L17601 (2007).
42. A. J. Cook, *et al.*, Atmospheric forcing of rapid marine-terminating glacier retreat in the Canadian Arctic Archipelago. *Sci. Adv.* **5**, 8507 (2019).
43. A. S. Gardner, M. Sharp, Influence of the Arctic Circumpolar Vortex on the mass balance of Canadian High Arctic glaciers. *J. Clim.* **20**, 4586–4598 (2006).
44. J. Zeeberg, S. L. Forman, Changes in glacier extent on north Novaya Zemlya in the twentieth century. *The Holocene* **11**, 161–175 (2001).
45. A. A. Bjørk, *et al.*, Changes in Greenland's peripheral glaciers linked to the North Atlantic Oscillation. *Nat. Clim. Chang.* **8**, 48–52 (2018).
46. V. Radić, *et al.*, Regional and global projections of twenty-first century glacier mass changes in response to climate scenarios from global climate models. *Clim. Dyn.* **42**, 37–58 (2014).
47. M. Möller, F. Navarro, A. Martín-Español, Monte Carlo modelling projects the loss of most land-terminating glaciers on Svalbard in the 21st century under RCP 8.5 forcing. *Environ. Res. Lett.* **11**, 094006 (2016).
48. E. M. Enderlin, *et al.*, An improved mass budget for the Greenland ice sheet. *Geophys. Res. Lett.* **41**, 866–872 (2014).

49. F. M. Nick, *et al.*, Future sea-level rise from Greenland's main outlet glaciers in a warming climate. *Nature* **497**, 235–238 (2013).
50. S. F. Price, A. J. Payne, I. M. Howat, B. E. Smith, Committed sea-level rise for the next century from Greenland ice sheet dynamics during the past decade. *Proc. Natl. Acad. Sci.* **108**, 8978–8983 (2011).

Deng, A., & Stauffer, D. R. (2006), On improving 4-km mesoscale model simulations. *Journal of Applied Meteorology and Climatology*, *45*(3), 361–381. doi:10.1175/JAM2341.1

More information on reference formatting with examples can be found in our Brief Guide to AGU Style.